Desalination and Water Treatment
www.deswater.com
doi: 10.1080/19443994.2013.867540

53 (2015) 844–852
January

Taylor & Francis
Taylor & Francis Group

Congo red removal using oxidized multiwalled carbon nanotubes: kinetic and isotherm study

Marjan Sheibani[a,*], Mehrorang Ghaedi[b], Farzaneh Marahel[a], Amin Ansari[a]

[a]*Department of Chemistry, Islamic Azad University, Omidiyeh Branch, Omidiyeh, Iran*
Tel. +98 652 3223434; Fax: +98 652 3222533; email: marjan.sheibani@gmail.com
[b]*Department of Chemistry, Yasouj University, Yasouj 75914-353, Iran*

Received 12 July 2013; Accepted 5 September 2013

ABSTRACT

In this study, Congo red (CR) was removed from aqueous solution by multiwalled carbon nanotube (MWCNT) oxidized and treated with HNO_3. In this regard, the influence of variables such as size and amount of MWCNT, pH, stirring time, and initial dye concentration on the procedure efficiency was examined and optimized. At optimum value of all variables, high adsorption capacity (357.14 mg g^{-1}) indicates the efficiency and suitability of MWCNT for achievement a safe and clean environment. The initial pH has significant role on the chemistry of dye molecules and adsorbent, and the best pH was 1.0. The removal rates follow the pseudo-second order in cooperate with interparticle diffusion models. The correlation coefficients were in the range of 0.9987–0.9998. The high adsorption capacities make MWCNT superior to activated carbon and admit to design safe, economic, and non-toxic wastewater treatment technology. The pH of zero charge of MWCNT was around 1.0. The higher the fraction of mesopores with size between 10 and 50 nm lead to enhance in the rate and amount of dyes adsorbed on its surface. Fitting the equilibrium adsorption data by Langmuir and Freundlich models shows that experimental data well explained by the by the Langmuir equation. The treated MWCNT has surface area, pore volume, and average pore diameter of 217.022 m^2/g, 0.757 cm^3/g, and 276.482 Å. The increase in the adsorption of the CR with rising temperature indicates its endothermic nature.

Keywords: Congo red; MWCNT; Kinetics and isotherm study

1. Introduction

Colored organic effluent is produced in industries such as textiles, rubber, paper, plastic, cosmetics, and dyes. Their discharge into water resources even in a small amount can affect the aquatic life and food web. Dyes lead to generation of allergic dermatitis, skin irritation and even may be carcinogenic and mutagenic for aquatic organisms. Dyes with synthetic origin and complex aromatic molecular structures are more stable, and their biodegradation is a difficult task [1]. Dyes classified as follows [2] anionic (direct, acid, and reactive dyes), cationic (basic dyes), and non-ionic (disperse dyes). Due to their low biodegradability, conventional biological wastewater treatment process is not very efficient wastewater treatment approach. Such media usually can be treated by physical- or chemical-treatment processes [3–7]. Adsorptions as one of the most effective and acceptable dye removal approaches are a well-known method especially based

*Corresponding author.

on application of low-cost adsorbents. The generally activated carbon with microporous structure has high surface area and efficiency for the adsorption of low molecular weight compounds, while fail to adsorb strongly giant molecules. The adsorption of bigger size compounds, such as dyes, dextrin, or natural organic materials, requires a material with high mesopore contribution to the total pore volume of adsorbent [8–11]. Most of the dyes can cause damage to aquatic life and human health that emerged from their toxicity, mutagenic, or carcinogenic nature [12]. Therefore, the removal of dyes from waste effluents has significant environmental importance [13]. Congo red (CR) (1-naphthalenesulfonic acid, 3,3-(4,4-biphenylenebis (azo))bis(4-amino-)disodium salt) is a benzidine-based anionic diazo dye [14] enter to various ecosystem from textiles, printing and dyeing, paper, rubber, and plastics wastewater [15]. This dye metabolizes to benzidine (known human carcinogen) that generates mutagen and reproductive effectors and also hazards for skin, eye, and gastrointestinal irritant [16]. Various adsorbents, especially nanomaterial-based adsorbents, proven to be promising effective material for the removal of various dyes [17–23]. In the present research, first various size multiwalled carbon nanotube (MWCNT) in the range of 8–15, 15–30, and > 50 nm was oxidized in the presence of nitric acid and subsequently applied for the dyes removal. The effect of factors such as initial pH (pH_0), adsorbent dose (m), contact time (t), initial concentration (C_0), and temperature (T) on CR removal percentage was investigated and optimized. The kinetics of adsorption using pseudo-first and second-order and diffusion models tested with experimental data for their validity. The equilibrium sorption behavior was examined by fitting the experimental data to various isotherm equations, and it was found that Langmuir is the best model with high correlation coefficient.

2. Materials and methods

2.1. Adsorbate

The adsorbate CR dye (C.I. = 22,120, chemical formula = $C_{32}H_{22}N_6Na_2O_6S_2$, FW = 696.7, λ_{max} = 500 nm) was supplied by S.D. Fine Chemicals, Mumbai, India. The dye was of analytical reagent grade and of 99.8% purity. The structure of CR is illustrated in Fig. 1. Stock solution (1,000 mg/L) of dye was prepared by dissolving an accurately weighed quantity of dye in double-distilled water. Experimental solutions of the desired concentrations were then obtained by its successive dilutions.

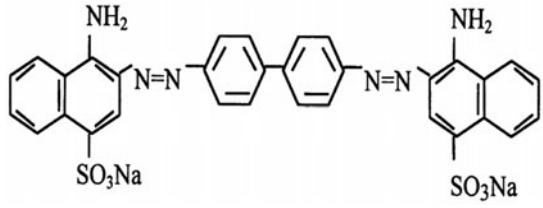

Fig. 1. Chemical structure of CR.

2.2. Analytical measurements

The CR in the aqueous solution was analyzed by UV spectrophotometer (Perkin–Elmer Lambda 35). The standard solutions at different pH values were scanned over 200–800 nm to determine the maximum absorbance wavelengths (λ_{max}). At these wavelengths, the calibration graphs were prepared, and accordingly the accurate determination of the CR residual was monitored.

2.3. Batch experimental program

Batch experiments were conducted to examine the effect of important parameters like initial pH (pH_0), adsorbent mass (m), initial concentration (C_0), and contact time (t) on the adsorptive removal of CR. For each experimental run, 50 mL of 20 mg L^{-1} of CR solution at various pH in the range of 1–7 was mixed thoroughly with 0.02 g of adsorbent. This mixture was agitated in a temperature-controlled vessel with constant speed of 150 rpm. Therefore, all the samples were centrifuged (Research centrifuge, Remi scientific works, Mumbai) at 4,000 rpm for 10 min to settle down suspended particles. After centrifugation, clear supernatant samples were obtained and the residual dye concentration was estimated accurately. The effect of pH in the range of 1–8 was studied, while the pH was adjusted by the addition of dilute aqueous solutions of H_2SO_4 and/or NaOH. The kinetics of adsorption was determined by analyzing adsorptive uptake of the dye from the aqueous solution at different time intervals. For adsorption isotherms, different concentration of dye solutions was agitated with known amount of adsorbent till the equilibrium. The effect of temperature on the sorption characteristics was investigated by determining the adsorption isotherms at 288 and 318 K. Blank experimental runs only the adsorbent in 50 mL of double-distilled water were conducted simultaneously at similar conditions to account for any color leached by the adsorbents and adsorbed by glass containers.

3. Results and discussion

3.1. Characterization of adsorbent

The MWCNT was oxidized according to our previous publications [5,7,23] as follows: MWCNT powder was purified and activated with 10% (v/v) hydrochloric acid solution for 24 h to remove adsorbed impurities and metal ions. Then, it was filtered, washed with distilled deionized water, and dried at 80°C for 5 h.

Subsequently was characterized by SEM and BET as shown in Figs. 2–6. The BET data are used to prove modification of the MWCNTs surface (Table 1). The IR spectrum of activated MWCNTs shows absorption frequencies at 3,400–3,600(bw), 1,627(s), 1,155(s), 673(s), and 592(s) cm^{-1} maybe assigned to stretching and bending of OH, C=O, C–O, and C=C groups. In preliminary experiments, various size of MWCNT was used for removal of CR from aqueous solution, and it was found that there is not significant change in removal percentages of CR until 50 nm (Table 2). Due to simple operation and easy phase separation, in this research for subsequent work, MWCNT with size in the range of 30–50 nm was selected as best adsorbent for efficient removal of present dye.

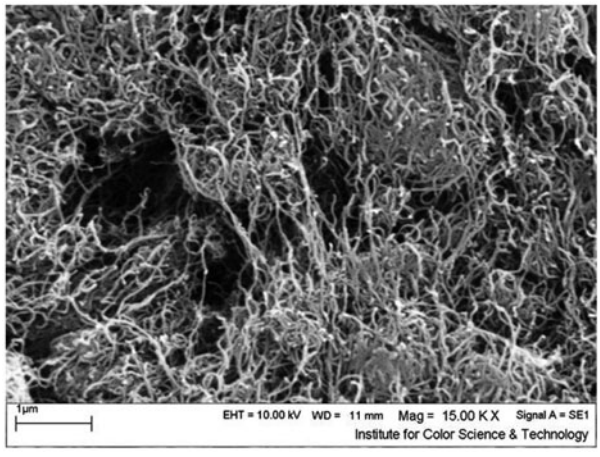

Fig. 2. SEM image of MWCNT.

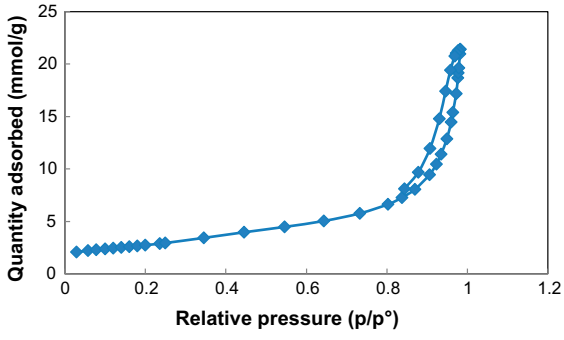

Fig. 3. Isotherm linear plot.

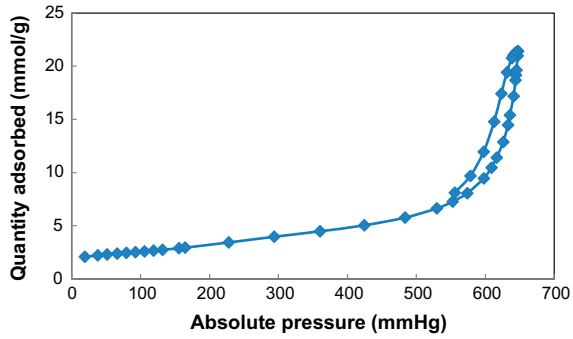

Fig. 4. Isotherm linear absolute plot.

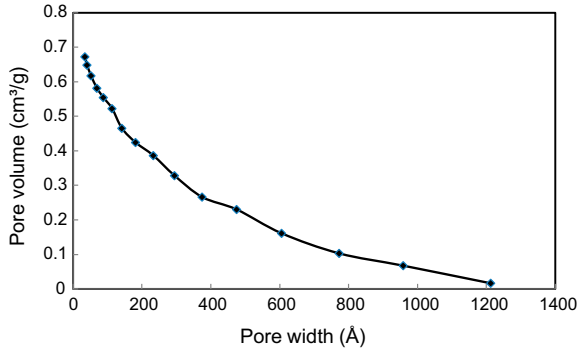

Fig. 5. BJH adsorption cumulative pore volume (Larger) Halsey: Faas correction.

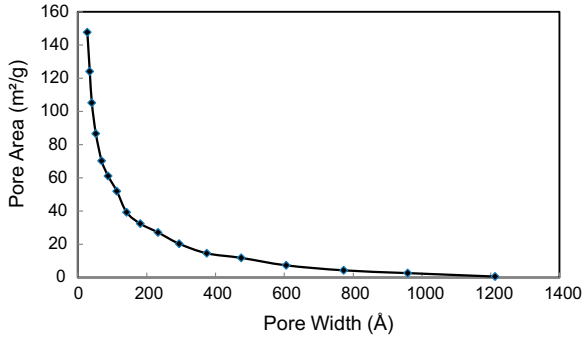

Fig. 6. BJH adsorption cumulative pore area (Larger) Halsey: Faas correction.

3.2. Effect of pH

The adsorptive treatment of dye containing wastewater is pH dependent. However, pH is also known

Table 1
Summary report of adsorbent properties

Summary report	
Surface area	
BET surface area:	217.0127 m^2/g
BJH adsorption cumulative surface area of pores between 17.000 Å and 3000.000 Å width:	230.787 m^2/g
BJH desorption cumulative surface area of pores between 17.000 Å and 3000.000 Å width:	243.6311 m^2/g
Pore volume	
BJH adsorption cumulative volume of pores between 17.000 Å and 3000.000 Å width:	0.756620 cm^3/g
BJH desorption cumulative volume of pores between 17.000 Å and 3000.000 Å width:	0.753632 cm^3/g
Pore size	
Adsorption average pore width (4 V/A by BET):	122.4743 Å
BJH adsorption average pore width (4 V/A):	131.137 Å
BJH desorption average pore width (4 V/A):	123.733 Å
Nanoparticle size	
Average particle size	276.482 Å

Table 2
Influences of size of MWCNT on CR removal percentages

MWCNT size	CR removal percentage (%)
<8	97
8–15	96
15–50	97
>50	92

to affect the structural stability of CR and its color intensity. Fig. 7 shows the CR removal trend from aqueous solution over a pH_0 range of 1–8. The effect of pH was studied with blank CR solutions (20 mg/L) with approximate natural pH_0 = 6.8. The solution was kept for 1 h after the pH adjustment and, subsequently, the absorbance of the solution was recorded. It is inferred that the CR solution is stable at pH around 1 and becomes unstable at both lower and higher pH. More than 90% of color removal is observed in the pH_0 range of 1–3. By raising the pH_0 from 2 to 7, the color removal decreases slightly from 80 to 65%. It can also be inferred from Fig. 7 that the CR removal is maximum at pH_0 = 1, and also the solution is most stable at this pH_0. Therefore, further adsorption experiments were carried out at pH_0 = 1. At lower pH due to the negative charge of CR and positive charge of oxidized MWCNT (protonation of the produced functional groups including hydroxide, carboxylic, and carbonyl), a strong electrostatic interaction enhance the removal percentage. At higher pH due to negative charge of both dye molecule and MWCNT surface lead to appearance of electrostatic repulsive force that hinders from dye adsorption.

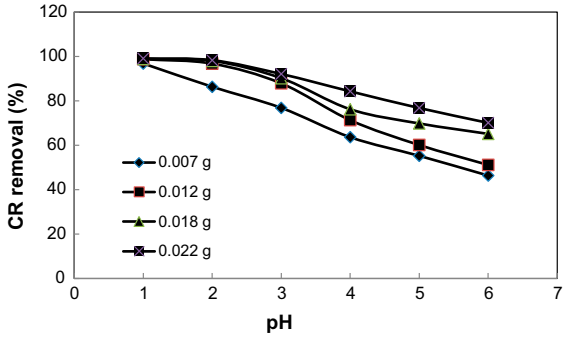

Fig. 7. Effect of system pH on adsorption of CR (20 mg L^{-1}) onto MWCNT (0.007–0.022 g) at room temperature (27 ± 2°C), agitation speed 300 rpm for the maximum contact time required to reach the equilibrium (20 min).

3.3. Effect of contact time (t) and initial dye concentration (C_0)

The effect of contact time on the CR removal at C_0 = 6, 12, 20, 30, and 40 mg/L (Fig. 8) was investigated, and it was found that rapid adsorption of CR occurs in the first 12 min. The increase in contact time up to 20 min shows that the CR removal increases slightly. It is mentionable that the difference in the adsorption values at 12 min and at 20 min is very small, and subsequently this contact time is steady state approximation and a quasi-equilibrium situation was accepted. Further experiments were conducted for 12 min contact time only. The effect of C_0 on the CR removal (Fig. 9) indicates that the CR percentage removal decreased with the increase in C_0. Although, CR adsorbed per unit mass of MWCNT (C_0) increased with the rise in C_0. The q_e enhances with the increase

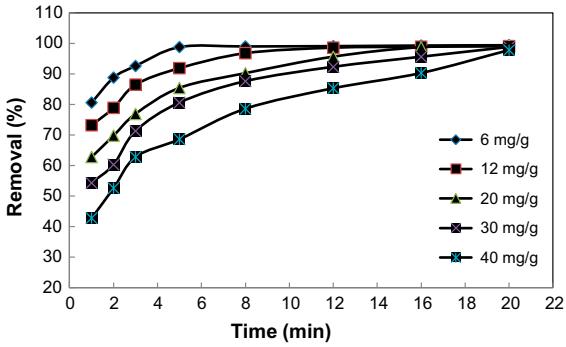

Fig. 8. Effect of contact time on the CR removal at 0.02 g adsorbent of MWCNT in different concentration (6–40 mg L^{-1}) of MG at pH 1.0.

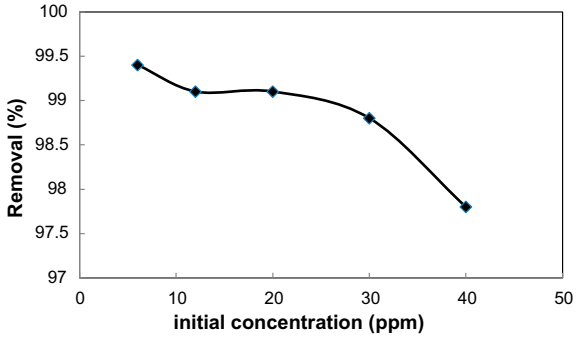

Fig. 9. Effect of initial dye concentration at 0.02 g adsorbent on the adsorption of CR.

in C_0 as the resistance to the uptake of CR from the solution decreases with the increase in CR concentration. The rate of adsorption also increases with the increase in C_0 due to increase in the driving force.

3.4. Effect of adsorbent dosage (m)

The effect of adsorbent mass on the uptake of CR onto adsorbent was studied at T = 30°C and C_0 = 5–55 mg/L and the results are shown in Fig. 10. The CR removal was increased with an increase in the adsorbent mass from 0.007 to 0.022 g, and it was observed that the removal remained unchanged for m > 0.022 g. The increase in the adsorption with adsorbent dosage can be attributed to the availability of greater surface area and more adsorption sites [24]. At m < 0.01 g, the MWCNT surface becomes saturated with CR, and the residual CR concentration in the solution is large. With an increase in m, CR removal increases due to enhance in the vacant adsorbent site. For m > 0.018 g, the incremental CR removal became low and at higher value, the removal efficiency becomes almost constant.

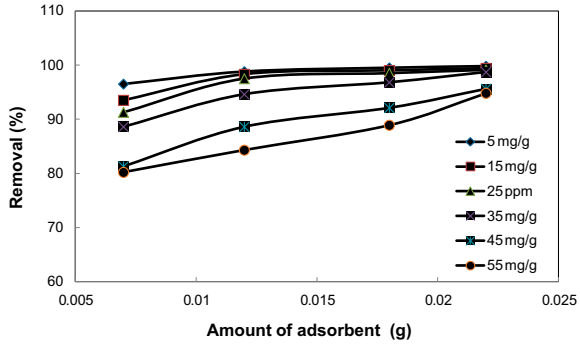

Fig. 10. Effect of adsorbent dosage on CR removals in the range of 0.007–0.022 g at (pH 1.0, agitation speed: 300 rpm, temperature: 27 ± 2°C).

3.5. Adsorption kinetic study

3.5.1. Pseudo-first-order and pseudo-second-order models

The adsorption of CR molecules from liquid phase to the solid phase can be considered as a reversible process. The uptake and retention of the CR molecules by adsorbent at any instant (t) is given as:

$$\log(q_e - q_t) = \log(q_e) - (K_1/2.303)t \quad (1)$$

where q_t is the amount of adsorbed compound at time t (mg/g), q_e is the adsorption capacity at equilibrium (mg/g), k_1 is the pseudo-first-order rate constant (min^{-1}), and t is the contact time (min). The pseudo-second-order model is represented as:

$$t/q_t = 1/k_2 q_e^2 + (1/q_e)t \quad (2)$$

The initial sorption rate, (h (mg/g min)), at $t \rightarrow 0$ initial rate is defined as:

$$h = k_2 q_e^2 \quad (3)$$

The prediction of the batch adsorption kinetics is necessary for the design of industrial adsorption columns. The experimental value of solid-phase concentration of adsorbate at equilibrium ($q_{e,exp}$) and the calculated value of solid-phase concentration of adsorbate at equilibrium ($q_{e,calc}$) for the pseudo-first-order model and pseudo-second-order models are presented in Table 3. The $q_{e,exp}$ and the $q_{e,calc}$ values from the pseudo-second-order kinetic model are very close to each other, and the coefficients of determination, (R^2), are also closer to unity for pseudo-second-order kinetics than for the pseudo-first-order kinetics.

Table 3
Kinetic parameters of CR removal using 0.015 g adsorbent over concentration in the range of 8–50 mg/L at optimal conditions

Parameter values: concentration dye (ppm)							
Models	Parameters	8	14	20	30	40	50
First-order-kinetic model: Log $(q_e - q_t) = \log(q_e) - (K_1/2.303)t$	K_1	0.245	0.196	0.145	0.105	0.086	0.067
	$q_{e,\ cal}$	15.84	19.6	29.6	48.9	59.8	68.6
	R^2	0.924	0.953	0.914	0.909	0.906	0.8911
Second-order-kinetic model: $t/q_t = 1/k_2 q_e^2 + (1/q_e)t$	$K_{2*}10^2$	0.182	0.145	0.109	0.087	0.053	0.023
	$q_{e,\ cal}$	29.8	41.6	59.9	78.9	118.6	138.9
	R^2	0.9997	0.9997	0.9998	0.9991	0.9987	0.9992
	H	53.8	76.9	112.7	162.9	206.3	229.7
Intraparticle diffusion $q_t = K_{id}\ t^{1/2} + C$	K_{dif}	1.9	3.8	6.8	9.6	14.6	18.9
	C	10.8	15.8	19.8	28.3	39.8	45.6
	R^2	0.816	0.857	0.881	0.875	0.846	0.893
Elovich $q_t = 1/\beta \ln(\alpha\beta) + 1/\beta \ln(t)$	β	0.083	0.156	0.198	0.245	0.298	0.364
	R^2	0.901	0.898	0.899	0.908	0.939	0.963
Experimental date	$q_{e,\ exp}$	32.6	42.8	60.6	79.8	120.3	141.2

Therefore, the sorption can be approximated more appropriately by the pseudo-second-order kinetic model than the first-order kinetic model for the adsorption of CR.

3.5.2. Weber–Morris intraparticle diffusion equation

The possibility of intraparticle diffusion was explored by using the intraparticle diffusion model [25]:

$$q_t = k_{id} t^{1/2} + C \tag{4}$$

where k_{id} is the intraparticle diffusion rate constant (mg/(g $min^{1/2}$)) and C (mg/g) is a constant. If the Weber–Morris plot of q_t vs. $t^{1/2}$ satisfies the linear relationship with the experimental data, then the sorption process is limited solely by intraparticle diffusion. The nonlinear nature of investigated line over the whole time range indicates contribution of more than one process in the sorption process. The independent of steps each other the plot of q_t vs. $t^{1/2}$ appears combination of two or more intersecting lines that show the first line represents surface adsorption and the second intraparticle diffusion. The presence of such distinctive features in the plots interpreted and belongs to the distinction between steps. Surface adsorption and intraparticle diffusion were likely to take place separately. The first portion (line not drawn for the clarity of picture) gives boundary layer diffusion, and further linear portions depict intraparticle diffusion. For C_0 = 8, 14, 20, 30, 40, and 50 mg/L, the first straight portion depicting mesopore diffusion, and the second line represents the micropore diffusion [26]. Extrapolation of the linear portions of the plots gives the intercepts and the value of I (the boundary layer thickness). The high value of intercept shows boundary layer dimension. The deviation of straight lines from the origin is obtained from difference in rate of mass transfer in the initial and final stages of adsorption. Deviation of straight line from the origin indicates the pore diffusion is not the sole rate controlling step [27]. Therefore, the adsorption proceeds via a complex mechanism. The values of $k_{id,1}$ and $k_{id,2}$ (obtained from the slopes of the straight lines) are presented in Table 3.

3.6. Adsorption equilibrium study

Various isotherm equations such as Freundlich, Tempkin, Dubinin–Radushkevich, and Langmuir were used to represent equilibrium adsorption data of target compounds on adsorbent. Despite serious limitations of all models that restrict their usage, the most popular Freundlich isotherm is suitable for highly heterogeneous surfaces. The Langmuir equation [28] is valid for homogeneous surfaces. The Tempkin isotherm contains a factor that explicitly takes into account the interactions between adsorbing species and the adsorbate. This isotherm assumes is based on linear reduce in adsorption of all heat with (adsorbate–adsorbate interactions) and according to uniform distribution of binding energies [29]. The Dubinin–Radushkevich (D–R) equation [30,31] is

Table 4
Isotherm constants of CR adsorption onto MWCNT

Isotherm	Equation		Parameters		Adsorbent (g)	
			0.007	0.012	0.018	0.022
Langmuir	$C_e/q_e = 1/K_aQ_m + C_e/Q_m$	Q_m (mg g^{-1})	357.14	200	76.33	65.79
		K_a (L mg^{-1})	0.021	1.47	4.85	8.94
		RL	0.90–0.46	0.12–0.012	0.04–0.003	0.022–0.002
		X^2	4.6	2.1	1.08	0.45
		R^2	0.9979	0.9942	0.9940	0.9891
Freundlich	$\ln q_e = \ln K_F + (1/n) \ln C_e$	$1/n$	0.53	0.42	0.33	0.35
		K_F (L mg^{-1})	95.81	92.86	59.9	55.38
		X^2	9.6	18.6	33.9	47.8
		R^2	0.9825	0.9235	0.9370	0.9454
Tempkin	$q_e = B_1 \ln K_T + B_1 \ln C_e$	B_1	66.4	34.27	12.43	11.08
		K_T (L mg^{-1})	6.90	28.74	106.74	172.53
		X^2	16.7	25.5	35.6	46.8
		R^2	0.9565	0.9653	0.9799	0.9810
Dubinin and Radushkevich	$\ln q_e = \ln Q_s - B\varepsilon^2$	Q_s (mg g^{-1})	215.64	150.20	64.06	57.36
		B	8E-08	4E-08	2E-08	1E-08
		E (kJ/mol) = $1/(2B)^{1/2}$	2.50	3.54	7.07	10.00
		X^2	106.6	143.7	289.6	371.9
		R^2	0.8528	0.9485	0.9761	0.9782

representing solute adsorption onto heterogeneous surfaces. The isotherm constants and correlation coefficient of Freundlich, Langmuir, Tempkin, and D–R isotherms models are listed in Table 4. Freundlich constants, K_F and $1/n$, indicate the adsorption capacity and adsorption intensity, respectively. Higher the value of $1/n$, the higher will be the affinity between the adsorbate and the adsorbent, and the heterogeneity of the adsorbent sites. The $1/n$ value indicates the relative distribution of energy sites and depends on the nature and strength of the adsorption process. The $1/n$ value of 0.53 refers to the fact that 90% of the active adsorption sites have equal energy level. Since $1/n < 1$, CR has favorable nature adsorption at all temperatures. The surface heterogeneity is due to the existence of crystal edges, type of anions, surface charges, and the degree of crystalline of the surface. The net effect of these factors is temperature dependent. The Freundlich isotherm does not predict the saturation of the adsorbent surface by the adsorbate. The K_F value can be taken as a relative indicator of the adsorption capacity [32,33]. The magnitude of K_F also showed the higher uptake of CR at higher temperature and endothermic nature of adsorption process. The maximum adsorption capacity of adsorbent (Q_s) is the monolayer saturation at equilibrium. The K_L value indicates the affinity of the CR to bind onto the adsorbent surface so that the higher K_L value indicates higher affinity. The D–R isotherm incorporates is applicable the homogenous and heterogeneous systems. The b value between 0 and 1 indicates favorable adsorption of CR onto adsorbent. The value of b helps in determining the mechanism of adsorption. A view glance to experimental results (Table 4) shows that b value closer to $[1 - (1/n)]$ vs. 1 show heterogeneous nature of adsorption. The comparison of the values of the error functions (Table 4) at all adsorbent dosages for all understudy isotherm models (Table 4) shows that the R^2 values for Langmuir model are closer to unity that shows its applicability for explanation of CR adsorption on this adsorbent.

4. Conclusion

This investigation shows the efficiency of MWCNT as a good, green, and low cost with high adsorption capacity (357.14 mg g^{-1}) adsorbent for the removal of CR from aqueous solutions in short time (<12 min). In this study, the effective pH was 1, and the optimum adsorbent dose was found to be 0.022 g. Langmuir isotherm gave a better fit to adsorption isotherms than Freundlich isotherm using linear and nonlinear methods. The kinetic study of CR on MWCNT was performed based on pseudo-first order, pseudo-second order, Elovich and intraparticle diffusion equations. The data indicate that the adsorption kinetics follow the pseudo-second-order rate in addition to inter particle diffusion.

References

[1] F. Taghizadeh, M. Ghaedi, K. Kamali, E. Sharifpour, R. Sahraie, M.K. Purkait, Comparison of nickel and/or zinc selenide nanoparticle loaded on activated carbon as efficient adsorbents for kinetic and equilibrium study of removal of Arsenazo(III) dye, Powder Technol. 245 (2013) 217–226.

[2] A. Mittal, V. Thakur, V. Gajbe, Evaluation of adsorption characteristics of an anionic azo dye brilliant yellow onto hen feathers in aqueous solutions, Environ. Sci. Pollut. Res. 19 (2012) 2438–2447.

[3] M. Ghaedi, F. Karimi, B. Barazesh, R. Sahraei, A. Daneshfar, Removal of reactive orange 12 from aqueous solutions by adsorption on tin sulfide nanoparticle loaded on activated carbon, J. Ind. Eng. Chem. 19 (2013) 756–763.

[4] M.K. Purkait, S.S. Vijay, S. Gupta, S. De, Separation of Congo red by surfactant mediated cloud point extraction, Dyes Pigm. 63 (2004) 151–159.

[5] A. Mittal, V. Thakur, V. Gajbe, Adsorptive removal of toxic azo dye amido black 10B by hen feather, Environ. Sci. Pollut. Res. 20 (2013) 260–269.

[6] M. Ghaedi, A. Hassanzadeh, S. Nasiri Kokhdan, Multiwalled carbon nanotubes as adsorbents for the kinetic and equilibrium study of the removal of alizarin red S and morin, J. Chem. Eng. Data 56 (2011) 2511–2520.

[7] F. Zhang, A. Yediler, X. Liang, A. Kettrup, Effect of dye additives on the ozonation process and oxidation byproducts: A comparative study using hydrolyzed C.I. reactive red 120, Dyes Pigm. 60 (2004) 1–7.

[8] M. Ghaedi, A. Shokrollahi, H. Hossainian, S. Nasiri Kokhdan, Comparison of activated carbon and multiwalled carbon nanotube for efficient removal of eriochrome cyanine R: Kinetic, isotherm and thermodynamic study of removal process, J. Chem. Eng. Data 56 (2011) 3227–3235.

[9] M. Ghaedi, Sh. Heidarpour, S. Nasiri Kokhdan, R. Sahraie, A. Daneshfar, B. Brazesh, Comparison of silver and palladium nanoparticles loaded on activated carbon for efficient removal of methylene blue: Kinetic and isotherm study of removal process, Powder Technol. 228 (2012) 18–25.

[10] A. Mittal, J. Damodar, J. Mittal, Adsorption of hazardous dye eosin yellow from aqueous solution onto waste material de-oiled soya: Isotherm, kinetics and bulk removal, J. Mol. Liq. 179 (2013) 133–140.

[11] M. Ghaedi, Comparison of cadmium hydroxide nanowires and silver nanoparticles loaded on activated carbon as new adsorbents for efficient removal of sunset yellow: Kinetics and equilibrium study, Spectrochim. Acta - Part A. 94 (2012) 346–351.

[12] Y. Yang, G. Wang, B. Wang, Z. Li, X. Jia, Q. Zhou, Biosorption of acid black 172 and Congo red from aqueous solution by nonviable penicillium YW 01: Kinetic study, equilibrium isotherm and artificial neural network modeling, Bioresour. Technol. 102 (2011) 828–832.

[13] C. Xia, Y. Jing, Y. Jia, D. Yue, J. Ma, X. Yin, Adsorption properties of Congo red from aqueous solution on modified hectorite: Kinetic and thermodynamic studies, Desalination 265 (2011) 81–87.

[14] V.K. Gupta, R. Jain, A. Mittal, S. Agarwal, S. Sikarwar, Photocatalytic degradation of toxic dye Amaranth on TiO_2/UV in aqueous suspensions, Mater. Sci. Eng. C 32 (2012) 12–17.

[15] I.D. Mall, V.C. Srivastava, N.K. Agarwall, I.M. Mishra, Removal of Congo red from aqueous solution by bagasse fly ash and activated carbon: Kinetic study and equilibrium isotherm analyses, Chemosphere 61 (2005) 492–501.

[16] B. Cheng, Y. Le, W. Cai, J. Yu, Synthesis of hierarchical Ni(OH)2 and NiO nanosheets and their adsorption kinetics and isotherms to Congo red in water, J. Hazard. Mater. 185 (2011) 889–897.

[17] A. Mittal, J. Mittal, A. Malviya, V.K. Gupta, Adsorptive removal of hazardous anionic dye "Congo red" from wastewater using waste materials and recovery by desorption, J. Colloid Interface Sci. 340 (2009) 16–26.

[18] V.K. Gupta, Suhas, Application of low-cost adsorbents for dye removal—A review, J. Environ. Manage. 90 (2009) 2313–2342.

[19] R. Ahmad, R. Kumar, Adsorptive removal of Congo red dye from aqueous solution using bael shell carbon, Appl. Surf. Sci. 257 (2010) 1628–1633.

[20] K. Nuithitikul, S. Srikhun, S. Hirunpraditkoon, Kinetics and equilibrium adsorption of basic green 4 dye on activated carbon derived from durian peel: Effects of pyrolysis and post treatment conditions, J. Taiwan. Inst. Chem. Eng. 41 (2010) 591–598.

[21] R.L. Tseng, F.C. Wu, R.S. Juang, Characteristics and applications of the Lagergren's first-order equation for adsorption kinetics, J. Taiwan. Inst. Chem. Eng. 41 (2010) 661–669.

[22] M. Benavente, L. Moreno, J. Martinez, Sorption of heavy metals from gold mining wastewater using chitosan, J. Taiwan. Inst. Chem. Eng. 42 (2011) 976–988.

[23] B.K. Nandi, A. Goswami, M.K. Purkait, Adsorption characteristics of brilliant green dye on kaolin, J. Hazard. Mater. 161 (2009) 387–395.

[24] E.P. Barret, L.G. Joyer, P.P. Halenda, The determination of pore volume and area distributions in porous substances. 1. Computations from nitrogen isotherms, J. Am. Chem. Soc. 73 (1951) 373–380.

[25] M. Ghaedi, M.N. Biyareh, S. Nasiri, S. Shamsaldini, R. Sahraei, A. Daneshfar, S. Shahriyar, Comparison of the efficiency of palladium and silver nanoparticles loaded on activated carbon and zinc oxide nanorods loaded on activated carbon as new adsorbents for removal of Congo red from aqueous solution: Kinetic and isotherm study, Mater. Sci. Eng. C 32 (2012) 725–734.

[26] J. Weber, J.C. Morris, Kinetics of adsorption on carbon from solution, J. Sanit. Eng. Div. 89 (1963) 31–59.

[27] U.R. Lakshmi, V.C. Srivastava, I.D. Mall, D.H. Lataye, Rice husk ash as an effective adsorbent: Evaluation of adsorptive characteristics for indigo carmine dye, J. Environ. Manage. 90 (2009) 710–720.

[28] A. Mittal, V.K. Gupta, Adsorptive removal and recovery of the azo dye eriochrome black T, Toxicol. Environ. Chem. 92 (2010) 1813–1823.

[29] I. Langmuir, The constitution and fundamental properties of solids and liquids, J. Am. Chem. Soc. 38 (1916) 2221–2295.

[30] M.I. Tempkin, V. Pyzhev, Kinetics of ammonia synthesis on promoted iron catalysts, Acta Physiochim. 12 (1940) 217–222.
[31] M.M. Dubinin, The potential theory of adsorption of gases and vapors for adsorbents with energetically non-uniform surface, Chem. Rev. 60 (1960) 235–266.
[32] L.V. Radushkevich, Potential theory of sorption and structure of carbons, Zh. Fiz. Khim. 23 (1949) 1410–1420.
[33] C. Namasivayam, D. Kavitha, Removal of Congo red from water by adsorption onto activated carbon prepared from coir pith, an agricultural solid waste, Dyes Pigm. 54 (2002) 47–58.